A novel 45-channel electron spectrometer for high intensity laser-plasma interaction studies

C. Gahn, G. D. Tsakiris, and K. J. Witte
Max-Planck-Institut für Quantenoptik, D-85748 Garching, Germany

P. Thirolf and D. Habs
Sektion Physik, LMU München, Am Coulombwall 1, D-85748 Garching, Germany

(Received 23 July 1999; accepted for publication 5 January 2000)

We have developed a magnetic spectrometer to characterize the hot electrons generated in high-intensity ($>10^{18}\,\mathrm{W/cm^2}$) laser-plasma interaction experiments. It comprises a dispersive element consisting of a permanent dipole magnet and an electron detector incorporating 45 scintillating/light-guiding plastic fibers connected to a cooled charged-coupled device camera. The main features of this instrument are high spectral resolution, low sensitivity to x and γ rays, and versatility due to its compact design. Performance and operational capabilities are illustrated based on experimental results in which electron energy–spectra in the range of 520 keV to 12.6 MeV were obtained with an energy resolution of 10% and a detection threshold of 10^6 electrons per MeV. © *2000 American Institute of Physics.* [S0034-6748(00)04804-8]

I. INTRODUCTION

Recently, the generation of multi-MeV electrons in the interaction of ultraintense laser pulses with plasma has attracted a lot of attention.[1–11] One key issue associated with this process is the mechanism leading to the acceleration of electrons to multi-MeV energies. In order to be able to elucidate this point, detailed information on their angular and energy distribution is necessary. A number of diagnostic techniques have been developed to obtain this information.[2–10] In most of these studies, an electron spectrometer was used in which the dispersive element was a static magnetic field while the detectors employed were of a different type. They included, for example, thick silicon diodes,[4] surface barrier detectors,[5] uncalibrated scintillating screens,[6] or combination of scintillators connected to photomultipliers.[5,10] In this article, we describe a new type of magnetic spectrometer in which the dispersive element (dipole magnet) and the electronic part of the detector are physically separated. The detector is an array of scintillating fibers and therefore, the number of channels and consequently the energy resolution is considerably increased compared to previous schemes.[4,5] The advantages of this design are compactness, suitability for operation in vacuum, and high energy resolution. Furthermore, since the electron detectors (scintillating fibers) discriminate against x and γ rays that are simultaneously generated to a large extent via Bremsstrahlung, the background signal in the output is rather low.

A schematic drawing of the spectrometer setup is shown in Fig. 1. The electrons pass through a collimator, which blocks the main part of the electron beam and through its aperture lets only a small fraction enter the permanent dipole magnet. Subsequently, they are dispersed according to their energy and those electrons striking the scintillating fibers produce a light signal that is proportional to their number in the respective energy range. The thus generated light signal is guided by total reflection in the fibers to a charge coupled device (CCD) camera where it is read out. A fiber optics window which is glued directly to the CCD chip provides the connection between the fiber ends and the chip. From the recorded image of the fiber array, the energy spectrum can be deduced. In what follows, the description and operational characteristics of the various components is explained in further detail.

A photograph of the partially dismantled spectrometer (without the collimator and with bare scintillating fibers) is shown in Fig. 2.

II. DISPERSIVE ELEMENT: DIPOLE MAGNET

The permanent dipole magnet utilized to disperse the electrons according to their kinetic energy consists of a top and a bottom array of magnets. Each array is composed of 25 pieces of 1-cm-thick ferrite permanent magnets placed on a 1-cm-thick iron plate and covered by a 3-mm-thick aluminum sheet. The dimensions of each pole face are 12.5 cm by 22.5 cm. The two poles are connected by a 1.5-cm-thick iron yoke providing a 1.5 cm gap between them. The overall height of the spectrometer is 6.5 cm. The magnetic field reaches a maximum field strength of 150 mT. It was mapped out with a Hall probe over a grid of $1\,\mathrm{cm}\times 1\,\mathrm{cm}$ lateral length. The projected electron trajectories were computed by ray tracing using a two-dimensional interpolation method for the magnetic field and calculating the deflection angle according to the Lorentz force [see Fig. 3(a)]. The dispersion relation deduced from these trajectories depends on the kinetic energy T and can be fitted by a function of the form $\Delta T/\Delta x = a + b\,T^c$, where a, b, and c are fitting parameters and x the distance along the dispersion direction [see Fig. 3(b)]. For an infinitely small aperture diameter, the theoretical energy resolution is $\Delta T/T = (d_f/T)\Delta T/\Delta x$ with d_f the fiber diameter. For $d_f = 1$ mm, this leads to a theoretical energy resolution of 1%–2% [see also Fig. 3(b)].

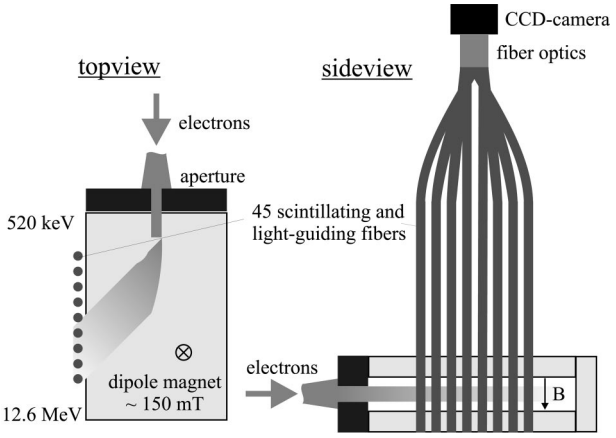

FIG. 1. Schematic of the electron spectrometer setup.

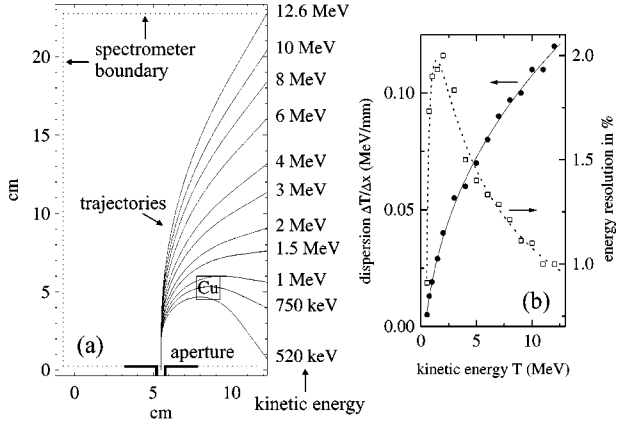

FIG. 3. (a) Electron trajectories in the magnetic spectrometer. The square with the label Cu indicates the position of the copper block used for noise measurements (see Sec. IV). (b) Dispersion relation (ray tracing results depicted by filled circles and fit by solid line, respectively) and energy resolution assuming an infinite small aperture (open squares and dotted line).

Depending on the collecting solid angle subtended by the entrance aperture the resolution worsens in the experiment due to the divergence of the incoming electron beam. In the case of the measurement described in Sec. IV, we used a 5 mm aperture that was placed 14 cm away from the interaction region resulting in an acceptance solid angle of 1 msr. This arrangement leads to an energy resolution of about 10%.

III. ELECTRON DETECTOR: SCINTILLATING FIBERS COUPLED TO A CCD CAMERA

The electrons are detected by round scintillating plastic fibers with 1 mm diameter. We chose these fibers for two reasons. First, they are made of a material with a low atomic number and consequently they are relatively insensitive to the x- and γ-ray background[12] copiously produced via Bremsstrahlung in this kind of experiment. Hence, a large-scale shielding of the detector is not required. Second, since these plastic fibers are very flexible, they allow easy repositioning of the spectrometer in the vacuum chamber. They are of the type BCF-12 manufactured by Bicron, Saint-Gobain Industrial Ceramics, Inc. Data concerning these fibers were taken from Ref. 13. They are equally spaced at the exit of the spectrometer and placed perpendicularly to the plane of the electron movement (see Fig. 1). The fiber bundle is 45 cm long and guides the scintillation light to the wall of the vacuum chamber where a 16-bit Photometrics CCD camera with a fiber optics interface is attached.[14] Their ends are glued in matrix arrangement into an aluminum plate using the optical cement Bicron BC-600 and the surface of the plate including the tips of the fibers are mechanically polished (see Fig. 2). This plate is slightly pressed against a fiber optics interface that is glued to the 1 in. CCD chip of type SIA003AF by Scientific Imaging Technologies, Inc.[15] A thin film of the silicon optical grease Bicron BC-630 is applied between mask and fiber optics. The refraction index of this grease comes close to the corresponding values for the fibers as well as for the fiber optics so that the light loss due to reflection at the interface between the end of the fibers and the fiber optics is reduced. The fibers are completely wrapped into black tape Bicron BC-638 in order to protect them against stray light.

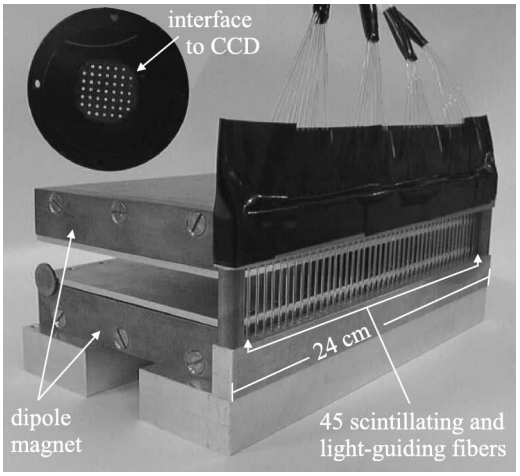

FIG. 2. Photograph of the electron spectrometer. The length of the fiber bundle is 45 cm.

When the dispersed electrons traverse these fibers, they deposit an amount of energy between 235 and 150 keV depending on their initial kinetic energy. These values were calculated by means of the Monte Carlo code GEANT,[16] a detector simulation tool originally designed for high-energy physics. The energy lost is converted into 8000 photons per MeV. About 4% of this light is funneled into the fiber by total internal reflection.[13,17] Due to absorption, with corresponding absorption $(1/e)$ length of 220 cm, 20% of this forward-coupled light is lost. Therefore, each electron gives rise to about 50 photons that reach the CCD camera. The chip has a mean quantum efficiency of 12% in the range of the spectrum that is emitted by the scintillation process. The mean photon energy of the spectrum is 2.8 eV. Moreover, an energy of 3.65 eV is required to create an electron-hole pair in a silicon semiconductor and the camera gain amounts to 5.1 electric charges per CCD count. Thus, on the whole each detected electron gives rise to 0.7–1.1 CCD counts depending on its kinetic energy. This value must be downgraded by about 25% as our absolute calibration with a ^{137}Cs β source revealed.

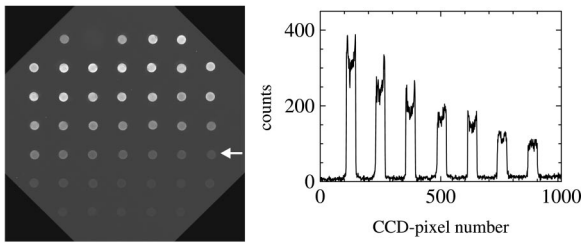

FIG. 4. Signals of the scintillating fibers recorded by the CCD camera: image (on the left) (the second fiber in the upper left corner is missing due to a misalignment during the gluing) and line-out of the row indicated by the white arrow (on the right).

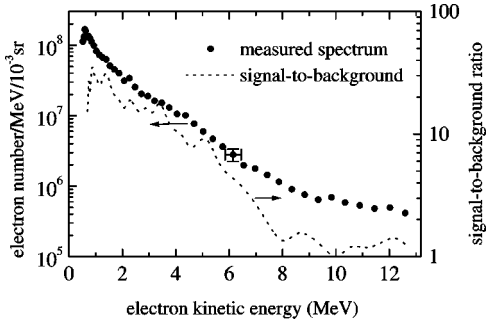

FIG. 5. Measured electron spectrum (dots) and signal-to-background ratio (dotted line).

Figure 4 shows an image recorded by the CCD camera in the experiment described in Sec. IV. The shining fiber ends can clearly be seen. The hollow structure seen in the line-out image of the individual fibers on the right is due to the light propagating characteristics in the multimode fiber. The lineout also indicates that the fibers are sufficiently well separated that crosstalk on the CCD chip can be excluded. Indeed, the crosstalk between adjacent fibers due to light escaping from one fiber and entering the other was found to be less than 5%. For this measurement we coupled two side by side lying fibers to a multichannel photomultiplier, placed ^{106}Ru β source on one fiber, and looked for coincident signals on both fibers using a gated analog-to-digital converter.

The data analysis is automated with a program on a dedicated PC that integrates the signal from the individual pixels within a square encircling each fiber.

IV. OPERATION IN A LASER-PLASMA EXPERIMENT

An experiment[11] in which the spectrometer described here played an important role was carried out using the advanced Ti:sapphire laser (ATLAS) at the Max-Planck-Institut für Quantenoptik that delivers 200 fs, 250 mJ pulses at 790 nm. The laser beam was focused with an $f/3$ off-axis parabolic mirror to a spot of 15 μm in diameter containing 85% of the total energy. The double-Gaussian intensity profile has a peak value of 4×10^{18} W/cm^2. The focus was placed at the edge of a free expansion argon gas jet provided by a high pressure gas nozzle of the type characterized in Ref. 18. The jet pressure reached a maximum of 0.5 bar.

The spectrometer was placed in laser beam direction 14 cm away from the interaction region. An aperture made of 8-mm-thick copper with a 5 mm hole collimated the electrons. A wall made out of 3 cm lead protected the fibers against direct bombardment by electrons outside of the spectrometer. In order to measure the signal caused by background radiation, the aperture was replaced by an identical piece of copper without a hole. Figure 5 shows a typical spectrum that we obtained after integrating over the pixels encircled by each fiber, subtracting the background from the signal and taking into consideration the dispersion relation given in Fig. 3 as well as the detector efficiency derived in Sec. III. The error bar for the electron number is associated with shot-to-shot fluctuations, the error bar for the kinetic energy is due to the angular spread of the electron beam (see Sec. II). In addition, the signal-to-background ratio is given. It reaches a maximum of 40 in the low energy part of the spectrum and drops to 1 in the high energy tail where the electron number is lower than 10^6 per MeV. By means of a small size copper block that was inserted into the spectrometer as shown in Fig. 3, we could estimate the influence of scattered electrons on the measured signal. Its position was such that it obstructed the lower part of the spectrum containing the electrons with an energy of up to 1 MeV, but allowed scattered electrons to access the blocked fibers. In fact, the signal was now reduced to the background level mentioned before. Since the plastic fibers are flexible, the spectrometer could be rotated horizontally as well as vertically around the interaction region up to an angle of 10° relative to the laser beam direction thus allowing measurements of the angular dependence of the electron energy distribution.

V. DISCUSSION

The usage of the spectrometer described here is not restricted to experiments of the above mentioned gas-jet type, but it can also be used in studies of laser interaction with solid targets. Modifications can be easily implemented to meet some special requirements associated with a specific experiment. For example, the number of energy channels available can be increased if an image reducer is used in connection with the CCD detector instead of a straight piece of fiber optics. In addition, if a different field strength of the dipole magnet is chosen, another part of the energy spectrum can be measured.

ACKNOWLEDGMENTS

This research was supported by the Commission of the EC within the framework of the Association Euratom—Max-Planck-Institut für Plasmaphysik and DFG Contract No. Ha-1101/7-1. The technical assistance of H. Haas, A. Böswald, and P. Sachsenmaier is greatly appreciated.

[1] G. A. Mourou, C. P. J. Barty, and M. D. Perry, Phys. Today **51**, 22 (1998).
[2] A. Modena, Z. Najmudin, A. E. Dangor, C. E. Clayton, K. A. Marsh, C. Joshi, V. Malka, C. B. Darrow, C. Danson, D. Neely, and F. N. Walsh, Nature (London) **377**, 606 (1995).
[3] D. Umstadter, S.-Y. Chen, A. Maksimchuk, G. Mourou, and R. Wagner, Science **273**, 472 (1996).
[4] G. Malka, J. Fuchs, F. Amiranoff, S. D. Baton, R. Gaillard, J. L. Miquel, H. Pépin, C. Rousseaux, G. Bonnaud, M. Busquet, and L. Lours, Phys. Rev. Lett. **79**, 2053 (1997).
[5] C. I. Moore, A. Ting, K. Krushelnick, E. Esarey, R. F. Hubbard, B. Hafizi,

H. R. Burris, C. Manka, and P. Sprangle, Phys. Rev. Lett. **79**, 3909 (1997).
[6] R. Wagner, S.-Y. Chen, A. Maksimchuk, and D. Umstadter, Phys. Rev. Lett. **78**, 3125 (1997).
[7] D. Gordon, K. C. Tzeng, C. E. Clayton, A. E. Dangor, V. Malka, K. A. Marsh, A. Modena, W. B. Mori, P. Muggli, Z. Najmudin, D. Neely, C. Danson, and C. Joshi, Phys. Rev. Lett. **80**, 2133 (1998).
[8] M. D. Perry, J. A. Sefcik, T. Cowan, S. Hatchett, A. Hunt, M. Moran, D. Pennington, R. Snavely, and S. C. Wilks, Rev. Sci. Instrum. **70**, 265 (1999).
[9] T. W. Phillips, M. D. Cable, T. E. Cowan, S. P. Hatchett, E. A. Henry, M. H. Key, M. D. Perry, T. C. Sangster, and M. A. Stoye, Rev. Sci. Instrum. **70**, 1213 (1999).
[10] F. Dorchies, F. Amiranoff, V. Malka, J. R. Marquès, A. Modena, D. Bernard, F. Jacquet, Ph. Miné, B. Cros, G. Matthieussent, P. Mora, A. Solodov, J. Morillo, and Z. Najmudin, Phys. Plasmas **6**, 2903 (1999).
[11] C. Gahn, G. D. Tsakiris, A. Pukhov, J. Meyer-ter-Vehn, G. Pretzler, P. Thirolf, D. Habs, and K. J. Witte, Phys. Rev. Lett. **83**, 4772 (1999).
[12] T. O. White, Nucl. Instrum. Methods Phys. Res. A **273**, 820 (1988).
[13] Bicron, Saint-Gobain Industrial Ceramics, Inc., *Product Lines*, online in Internet:http://www.bicron.com/prod.htm (1999).
[14] Photometrics GmbH, *Photometrics Series 300*, online in Internet: www.photometrics.de/S300.html (1999).
[15] Scientific Imaging Technologies, Inc., *Products*, online in Internet: http://www.site-inc.com/products.htm (1999).
[16] *GEANT User's Guide*, edited by R. Brun, M. Hansroul, and J. C. Lassalle, CERN Report No. DD/EE/82 (1982).
[17] W. R. Binns, M. H. Israel, and J. Klarmann, Nucl. Instrum. Methods Phys. Res. **216**, 475 (1983).
[18] Y. M. Li and R. Fedosejevs, Meas. Sci. Technol. **5**, 1197 (1994).